Cellular/Molecular

Unraveling the High- and Low-Sensitivity Agonist Responses of Nicotinic Acetylcholine Receptors

Kasper Harpsøe,[1]* Philip K. Ahring,[2]* Jeppe K. Christensen,[2] Marianne L. Jensen,[2] Dan Peters,[2] and Thomas Balle[1]

[1]Department of Medicinal Chemistry, Faculty of Pharmaceutical Sciences, University of Copenhagen, DK-2100 Copenhagen, Denmark, and [2]NeuroSearch A/S, DK-2750 Ballerup, Denmark

The neuronal $\alpha4\beta2$ nicotinic acetylcholine receptors exist as two distinct subtypes, $(\alpha4)_2(\beta2)_3$ and $(\alpha4)_3(\beta2)_2$, and biphasic responses to acetylcholine and other agonists have been ascribed previously to coexistence of these two receptor subtypes. We offer a novel and radical explanation for the observation of two distinct agonist sensitivities. Using different expression ratios of mammalian $\alpha4$ and $\beta2$ subunits and concatenated constructs, we demonstrate that a biphasic response is an intrinsic functional property of the $(\alpha4)_3(\beta2)_2$ receptor. In addition to two high-sensitivity sites at $\alpha4\beta2$ interfaces, the $(\alpha4)_3(\beta2)_2$ receptor contains a third low-sensitivity agonist binding site in the $\alpha4\alpha4$ interface. Occupation of this site is required for full activation and is responsible for the widened dynamic response range of this receptor subtype. By site-directed mutagenesis, we show that three residues, which differ between the $\alpha4\beta2$ and $\alpha4\alpha4$ sites, control agonist sensitivity. The results presented here provide a basic insight into the function of pentameric ligand-gated ion channels, which enables modulation of the receptors with hitherto unseen precision; it becomes possible to rationally design therapeutics targeting subpopulations of specific receptor subtypes.

Introduction

The nicotinic acetylcholine receptors (nAChRs) are members of the Cys-loop receptor family of pentameric ligand-gated ion channels. The neuronal $\alpha4\beta2$ receptor is widely distributed in the mammalian brain and thought to be responsible for nicotine addiction and to play a central role in several psychiatric and neurodegenerative disorders (Jensen et al., 2005), which makes it a highly important therapeutic target.

$\alpha4$ and $\beta2$ subunits can assemble with different stoichiometries to form two distinct functional receptor subtypes, $(\alpha4)_2(\beta2)_3$ and $(\alpha4)_3(\beta2)_2$ (Nelson et al., 2003; Moroni et al., 2006). Both subtypes may be pharmacologically important because they seem to be present in native brain (Marks et al., 2007) and they display significantly different physiological properties (Nelson et al., 2003; Kuryatov et al., 2005; Moroni et al., 2006, 2008; Tapia et al., 2007). Expressing $\alpha4$ and $\beta2$ subunits in equal amounts in oocytes gives rise to a receptor population, resulting in biphasic concentration–response curves to the endogenous ligand acetylcholine (ACh) and other agonists. The different agonist sensitivities are clearly related to the subunit stoichiometry, and, based on studies with different $\alpha4$:$\beta2$ expression ratios and concatenated subunits (Nelson et al., 2003; Zhou et al., 2003; Kuryatov et al., 2005; Moroni et al., 2006; Zwart et al., 2006; Carbone et al., 2009), the high- and low-sensitivity components of the biphasic curves have been ascribed to the $(\alpha4)_2(\beta2)_3$ and $(\alpha4)_3(\beta2)_2$ receptor subtypes, respectively. Although mixtures of different stoichiometries can explain biphasic concentration–response curves, the lack of a detailed explanation for the different agonist sensitivities has made interpretation of certain experimental data difficult and has hampered rational drug design. Hence, a thorough understanding of the underlying mechanism is highly desirable and may be relevant to other Cys-loop receptors, including the major ganglionic nAChR $\alpha3\beta4$ subtype, which also assemble in two different stoichiometries (Krashia et al., 2010).

On the subunit level (Fig. 1*A*), both receptor subtypes comprise two $\alpha4\beta2$ interfaces known to bind ACh. However, the $(\alpha4)_3(\beta2)_2$ receptor contains a unique $\alpha4\alpha4$ interface, which we hypothesized to comprise a low-sensitivity agonist site. If agonist binding in the $\alpha4\alpha4$ interface is necessary to obtain full activation of the $(\alpha4)_3(\beta2)_2$ receptor, this offers an explanation for the observed lower agonist sensitivity.

We constructed and compared homology models of $\alpha4\alpha4$ and $\alpha4\beta2$ dimers and identified three differing key amino acids that likely affect agonist binding. We then introduced mutations in the $\alpha4\beta2$ receptor to convert the low-sensitivity $\alpha4\alpha4$ site into a high-sensitivity $\alpha4\beta2$-like site and vice versa to investigate whether these sites are responsible for the observed agonist sensitivities. The mutant and wild-type $\alpha4$ and $\beta2$ subunits were expressed in different ratios in oocytes and tested with ACh and a partial agonist 1-(5-ethoxypyridin-3-yl)-1,4-diazepane (NS3573) (Peters et al., 1999) (Fig. 1*B*). Collectively, all our data are con-

Received March 25, 2011; revised May 11, 2011; accepted May 27, 2011.

Author contributions: K.H., P.K.A., and T.B. designed research; K.H., P.K.A., and M.L.J. performed research; D.P. contributed unpublished reagents/analytic tools; K.H., P.K.A., J.K.C., and T.B. analyzed data; K.H., P.K.A., and T.B. wrote the paper.

*K.H. and P.K.A. contributed equally to this work.

The authors declare no competing financial interests.

This work was supported in part by grants from the Lundbeck Foundation (T.B.), the Carlsberg Foundation (T.B., K.H.), and the Drug Research Academy, Faculty of Pharmaceutical Sciences, University of Copenhagen (K.H.). We thank Camilla Irlind and Lene G. Larsen from NeuroSearch A/S for expert technical assistance.

Correspondence should be addressed to Thomas Balle, Department of Medicinal Chemistry, Faculty of Pharmaceutical Sciences, University of Copenhagen, DK-2100 Copenhagen, Denmark. E-mail: tb@farma.ku.dk.

DOI:10.1523/JNEUROSCI.1509-11.2011

 0270-6474/11/3110759-08$15.00/0

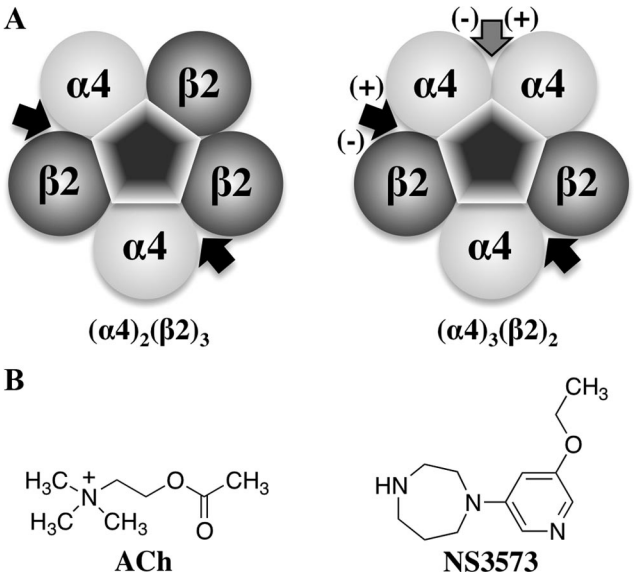

Figure 1. The $\alpha4\beta2$ nAChR subtypes and the agonists used. ***A***, Diagram of the $(\alpha4)_2(\beta2)_3$ and $(\alpha4)_3(\beta2)_2$ subtypes showing arrangement of subunits and location of agonist binding sites. The black arrows show the position of the confirmed orthosteric binding sites, and the gray arrow show the position of the hypothesized third agonist site of the $(\alpha4)_3(\beta2)_2$ subtype. (+) and (−) refers to the principal and complementary components of the binding sites. ***B***, Chemical structures of the endogenous ligand for $\alpha4\beta2$ receptors, ACh, and a partial agonist, NS3573.

sistent with a third binding site in the $\alpha4\alpha4$ interface and show biphasic concentration–response behavior as an intrinsic property of the $(\alpha4)_3(\beta2)_2$ receptor.

Materials and Methods

Homology models. The sequences of the ligand binding domain of α4 and β2 were retrieved from the Protein Knowledgebase (The UniProt Consortium, 2011; www.uniprot.org), entries P43681 and P17787, respectively. The structures and sequences of the templates were downloaded from The Protein Data Bank (PDB) (Berman et al., 2000) (www.pdb.org): the mouse α1 nAChR ligand binding domain with a toxin bound (PDB code 2QC1) (Dellisanti et al., 2007), ACh binding protein (AChBP) with nicotine bound (PDB code 1UW6) (Celie et al., 2004), and AChBP with epibatidine bound (PDB code 2BYQ) (Hansen et al., 2005). Preparation of the templates was performed by manual deletion of unwanted protein chains, residues, and heteroatom molecules. The alignment of the target and template sequences were initially created with EXPRESSO (Armougom et al., 2006) and then manually edited according to the following considerations: all three templates were used in regions with structural similarity, and otherwise 2QC1 were the template of choice excluding regions and residues that are structurally different as a result of the bound antagonist or mutated residues. The alignment with specification of which templates were used in certain regions is depicted in Figure 2. The homology models were prepared with MODELLER release 9v7 (Sali and Blundell, 1993), and nicotine was included in the dimer interface from the 1UW6 template. We built 100 models for each dimer and selected the best scoring models using the Discrete Optimized Protein Energy (DOPE) score (Shen and Sali, 2006) included in MODELLER. The selected $\alpha4\beta2$ and $\alpha4\alpha4$ models were imported into PyMOL (DeLano, 2002) and overlaid by superimposing the chains that make up the (−)-side of the binding site.

Preparation of wild-type, mutants, and concatenated α4 and β2 subunits. cDNA encoding human nAChR α4 and β2 subunits were cloned, and cRNA was prepared as described previously (Timmermann et al., 2007). The triple-point-mutated $\beta2^m$ subunit with the mutations V136H, F144Q, and L146T was constructed by site-directed mutagenesis using uracilated β2 containing plasmid as template and a 5′-phosphorylated primer of sequence: CCTTCTATTCCAATGCgcacGTCTCCTATGATGGCAGCATCcagTGGacGCCGCCTGCCATCTAC (small letters indicate mutations) as described previously (Jensen et al., 2002). The triple-point-mutated $\alpha4^m$ subunit with the mutations H142V, Q150F, and T152L was constructed by performing a restriction–ligation cycle substituting a large part of the N-terminal domain coding region with a ~430-bp-long synthetic DNA piece purchased from GenScript using the HinDIII site in position 288 and a previously introduced SalI site in position 717.

The nAChR β2-6-α4 concatamer (Zhou et al., 2003) was constructed by introducing half-parts of a linker sequence that contains an SacII restriction site into the 3′ end of β2 and the 5′ end of α4. The complete 20 aa linker sequence consist first of EG and then six in-frame AGS repeats (hence the "-6-" in the construct name) replacing the stop codon in β2 and the 24 aa signal peptide in the α4 subunit. Two primers were used for PCR reactions each with approximately a half part of the final linker: the β2 antisense primer sequence was gaattcgatcccgcggacccggcactgcctgcaccttcCTTGGAGCTGGGGGCTG, and the α4 sense primer sequence was cggatcctccgcgggaagtgctggaagtgctggaagtgctggaagtCGGGCCCACGCCGAGGAG (linker sequence written with small letters). After the PCR reactions, $\beta2^{3'\text{-Linker}}$ and $\alpha4^{5'\text{-Linker}}$ subunit intermediates were constructed, and the final concatamer was assembled using the unique SacII site in the linker sequence.

The nAChR β2-6-α4-9-β2-6-α4 concatamer was constructed in a manner similar to that described for the β2-6-α4 concatamer but this time using the β2-6-α4 concatamer itself as template for introducing half-parts of a linker. The 28 aa linker consisted of 9 (hence the "-9-" in the construct name) in-frame AGS repeats separated by an "extra" threonine residue between repeats 5 and 6 to introduce a SalI site and replaces the stop codon in the C terminus of β2-6-α4 and 25 aa signal peptide in the N terminus of β2-6-α4. The antisense primer used for a PCR reaction was ggcggccgcgtcgaccgcagacaccccgcgctacctgcggatccagcactacctgcGATCATGCCAGCCAGCCAGG, and the sense primer used for the second PCR reaction was tggtaccgtcgacggctggaagcgcaggtagtgctggcagtgcaggttcgACGGATACAGAGGAGCGGCT (linker sequence written with small letters). The final β2-6-α4-9-β2-6-α4 concatamer was constructed by ligation of the two intermediates $\beta2\text{-}6\text{-}\alpha4^{3'\text{-Linker}}$ and $\beta2\text{-}6\text{-}\alpha4^{5'\text{ Linker}}$ using the unique SalI site in the linker.

All constructs were verified by sequencing (MWG Biotech). Primers and oligos for mutations were purchased from MWG Biotech. Expand HF polymerase was from Roche Diagnostics. Restriction enzymes, T7 DNA polymerase, and T4 DNA ligase was from New England Biolabs. *Escherichia coli* XL1-Blue was from Stratagene. DNA purification kits were from Qiagen.

Oocyte preparation and electrophysiology. Xenopus laevis oocyte preparation and electrophysiological experiments were performed as described previously (Mirza et al., 2008). Briefly, lobes from ovaries of female adult *X. laevis* were removed and defolliculated to obtain isolated oocytes. Oocytes were injected with a total of ~25 ng of cRNA encoding human wild-type, mutant, or concatenated subunits (α4, β2, $\alpha4^m$, $\beta2^m$, β2-6-α4, or β2-6-α4-9-β2-6-α4) in the ratios stated in Table 1 and incubated 2–7 d at 15–18°C. Oocytes were subjected to two-electrode voltage-clamp electrophysiological testing using a custom-built system in which solutions were applied directly to the oocytes via a glass capillary tube placed in the vicinity of the cell to ensure a solution exchange rate in the order of a few seconds. Each application of ACh or NS3573 lasted ~1 min, and peak current amplitudes were measured. The protocol included dynamic adjustments of washing periods between applications to ensure full recovery at higher agonist concentrations.

Data management and statistical analysis. Full concentration–response datasets for ACh were fitted using GraphPad Prism 4 to either a monophasic $[I = I_{max}/(1 + 10^{(\log EC50 - [ACh])})]$ or biphasic $[I = I_{max} * \text{Frac}/(1 + 10^{(\log EC50\_1 - [ACh])}) + I_{max} * (1 - \text{Frac})/(1 + 10^{(\log EC50\_2 - [ACh])})]$ Hill equation, and the fitted maximal values ($I_{max\ fit\ ACh}$) were used for normalization of each dataset. In a similar manner, full concentration–response datasets for NS3573 were normalized to a maximal ACh stimulation ($I_{max\ ACh}$) on the same oocyte and then fitted to Hill equations as described above. GraphPad Prism 4 best-model *F* test was used to evaluate whether a given dataset was best represented by a biphasic or simpler monophasic model, and the results are written as *F* value (DFn, DFd).

To compare fractions of high-sensitivity component among biphasic fits, the fraction was determined for each single concentration–response

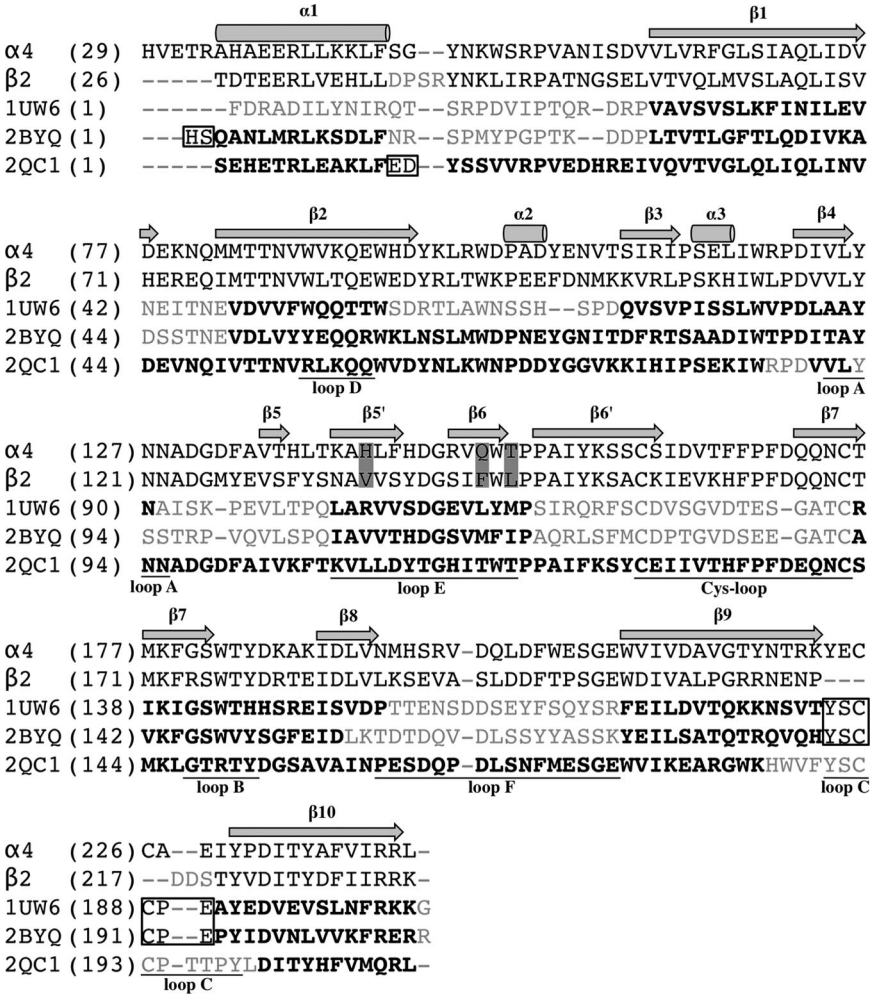

Figure 2. Sequence alignment used for homology modeling. The multi-template sequence alignment of $\alpha4$ and $\beta2$ to the three templates used to construct the dimeric $\alpha4\alpha4$ and $\alpha4\beta2$ homology models. The residues shown in bold were used as templates for modeling both $\alpha4$ and $\beta2$, whereas framed residues were used only for $\alpha4$. Residues that were not modeled on a template or not used as template are shown in gray. Numbering follows the PDB files for 1UW6 (AChBP with nicotine bound), 2BYQ (AChBP with epibatidine bound), and 2QC1 (mouse $\alpha1$ nAChR ligand binding domain with toxin bound) and is according to P43681 and P17787 at www.uniprot.org for $\alpha4$ and $\beta2$, respectively. The mutated residues are on a gray background, the secondary structure is indicated above the sequences, and the classical notation of the binding site regions (loops A–F) is given below the sequences.

dataset using biphasic fitting and the fraction means were statistically compared using GraphPad Prism 4 one-way ANOVA. For comparing EC_{50} values, GraphPad Prism 4 unpaired two-tailed *t* test was used.

Results

Structural comparison of binding sites and mutant design

To compare the putative agonist binding site in the $\alpha4\alpha4$ interface with the known binding site in the $\alpha4\beta2$ interfaces, we constructed homology models of the two dimers. As templates, we used crystal structures of the monomeric mouse nAChR $\alpha1$ subunit (Dellisanti et al., 2007), and the homologous AChBPs from *Lymnaea stagnalis* and *Aplysia californica* cocrystallized with the well-known $\alpha4\beta2$ agonists nicotine (Celie et al., 2004) and epibatidine (Hansen et al., 2005). Nicotine was included in the homology models during the model building procedure, and residues within 5 Å and with side chains pointing toward nicotine were defined as binding site residues. A superimposition of the two homology models showed that only three binding site residues on the (−)-side of the interface differ between the two sites (Fig. 3). The three residues are His142, Gln150, and Thr152 in $\alpha4$ and Val136, Phe144, and Leu146 in $\beta2$ (see also the alignment in Fig. 2), signifying a local change of the binding site from hydrophilic in an $\alpha4\alpha4$ interface to hydrophobic in an $\alpha4\beta2$ interface. To be able to convert the $\alpha4\alpha4$ site to resemble a $\alpha4\beta2$ site and vice versa, we constructed two triple mutants: $\alpha4$[H142V/Q150F/T152L] ($\alpha4^m$) and $\beta2$[V136H/F144Q/L146T] ($\beta2^m$).

Expression of $(\alpha4)_2(\beta2)_3$ and $(\alpha4)_3(\beta2)_2$ receptor subtypes

Initially, we expressed wild-type $\alpha4$ and $\beta2$ subunits in oocytes in 1:4 and 4:1 ratios to obtain $(\alpha4)_2(\beta2)_3$ and $(\alpha4)_3(\beta2)_2$ receptors, respectively, and conducted concentration–response experiments on the resulting receptor populations with ACh and NS3573. As seen from the representative traces for ACh and NS3573 experiments (Fig. 4), a full concentration–response dataset is obtained from each oocyte. In general, we observe lower current amplitudes from receptors expressed with excess $\beta2$ subunits (Fig. 4*A*) and higher current amplitudes with a surplus of $\alpha4$ subunits (Fig. 4*B*). Furthermore, when $\beta2$ is in excess, ACh and NS3573 yield concentration–response data that fit very well to a monophasic Hill equation, indicating a uniform $(\alpha4)_2(\beta2)_3$ receptor population (Fig. 5*A*,*C*; Table 1). The 1.6 μM potency of ACh is similar to previously reported values for $(\alpha4)_2(\beta2)_3$ receptors in oocytes (Moroni et al., 2006; Zwart et al., 2006; Carbone et al., 2009), whereas the 23 nM potency shows that NS3573 is a highly potent $\alpha4\beta2$ receptor agonist.

Concentration–response data obtained from the receptor population expressed with excess $\alpha4$ were significantly better fitted to a biphasic than a monophasic Hill equation (Fig. 5*A*,*C*; Table 1), yielding both a high- and low-sensitivity component for ACh (EC_{50_1} = 0.95 μM, EC_{50_2} = 83 μM) and NS3573 (EC_{50_1} = 9.8 nM, EC_{50_2} = 7.9 μM). The high-sensitivity potencies match those observed for the $(\alpha4)_2(\beta2)_3$ receptors, whereas the low-sensitivity potency for ACh matches previously described values for $(\alpha4)_3(\beta2)_2$ receptors expressed in oocytes (Moroni et al., 2006; Zwart et al., 2006; Carbone et al., 2009). The biphasic curves could be explained either as an inherent feature of the $(\alpha4)_3(\beta2)_2$ receptor, resulting from the presence of two different agonist binding sites, or it could indicate a non-uniform $(\alpha4)_3(\beta2)_2$ receptor population containing a small amount of $(\alpha4)_2(\beta2)_3$ receptors.

Biphasic response from the $(\alpha4)_3(\beta2)_2$ receptor

To investigate whether the biphasic concentration–response curves obtained from the $(\alpha4)_3(\beta2)_2$ would change with varying $\alpha4$:$\beta2$ expression ratios, we expressed $\alpha4$ and $\beta2$ subunits in oocytes in 20:1 and 100:1 ratios and collected concentration–response data for ACh and NS3573. As for the 4:1 expression ratios, a biphasic Hill equation gave best fits (Fig. 6*A*,*B*,*E*,*F*; Table 1), and the fractions between the high-sensitivity and low-

Table 1. Concentration–response data for ACh and NS3573 on wild-type, mutant, and concatenated α4β2 receptors expressed with different subunit ratios

			ACh					NS3573				
Subunits	Ratio	I_{max} (nA)[a]	EC_{50_1} (μM)[b]	EC_{50_2} (μM)[b]	Frac.[c]	n[d]	*F* value (DFn, DFd)[e]	EC_{50_1} (nM)[b]	EC_{50_2} (μM)[b]	Frac.[c]	*n*[d]	*F* value (DFn, DFd)[e]
α4:β2	1:4	920	1.6			6		23			20	
α4:β2	4:1	3800	0.95	83	0.16	17	38 (2,197)	9.8	7.9	0.24	24	31 (2,279)
α4m:β2	1:4	360	0.97			7		20			7	
α4m:β2	4:1	1400	3.2			8		22			8	
α4m:β2	100:1	1500	3.8			9		27			10	
α4:β2m	4:1	6600		140		7			23		11	
α4:β2	20:1	2900	1.4	141	0.14	20	58 (2,216)	4.4	10	0.26	14	63 (2,131)
α4:β2	100:1	2700	1.9	170	0.15	24	80 (2,284)	4.0	4.0	0.24	12	42 (2,138)
α4:β2-6-α4	1:1	2400	1.3	130	0.21	10	47 (2,116)	6.3	6.3	0.23	5	12 (2,56)
α4:β2-6-α-9-β2-6-α4	1:1	3300	2.5	130	0.24	8	42 (2,80)	5.0	7.9	0.26	9	64 (2,103)
β2-6-α-9-β2-6-α4:β2	1:1	290	1.3			12		18			13	

[a]Average of maximal ACh-evoked current amplitudes in *X. laevis* oocyte experiments. Oocytes were clamped at holding potentials ranging from −40 to −100 mV. Peak ACh_{max}-evoked current amplitudes from each experiment were recorded and baseline subtracted. Average current levels for all experiments on a given receptor population were rounded off to two significant digits, and SEM values were typically 10%.

[b]EC_{50_1} and EC_{50_2} correspond to the high- and low sensitivity potencies observed from the wild-type α4β2 in a 4:1 ratio, respectively.

[c]Fraction of the high-sensitivity component on receptors resulting in biphasic activation profiles.

[d]Number of experiments behind the data.

[e]For the experiments in which data were best fitted to biphasic Hill equations, the results from the best-model *F* test with $p < 0.0001$ are given as follows: *F* value (degrees of freedom for the numerator, degrees of freedom for the denominator).

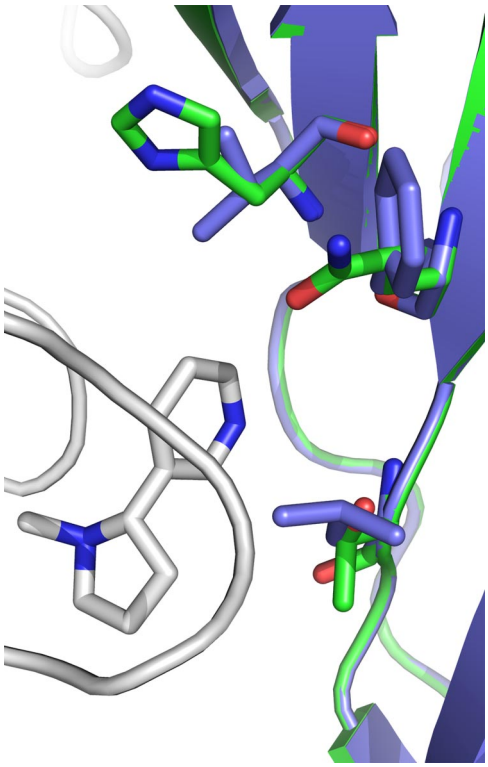

Figure 3. Structural comparison of the α4β2 and α4α4 sites. Superimposition of the homology models of the α4β2 and α4α4 dimers with the protein backbone represented as cartoon, whereas nicotine and the three residues that differ between the sites are shown as sticks. From the top, these residues are His142, Gln150, and Thr152 in α4 (green carbon atoms) and Val136, Phe144, and Leu146 in β2 (slate carbon atoms). The identical (+)-side of the binding sites and nicotine are colored with white carbons and for clarity reasons only displayed from the α4α4 homology model.

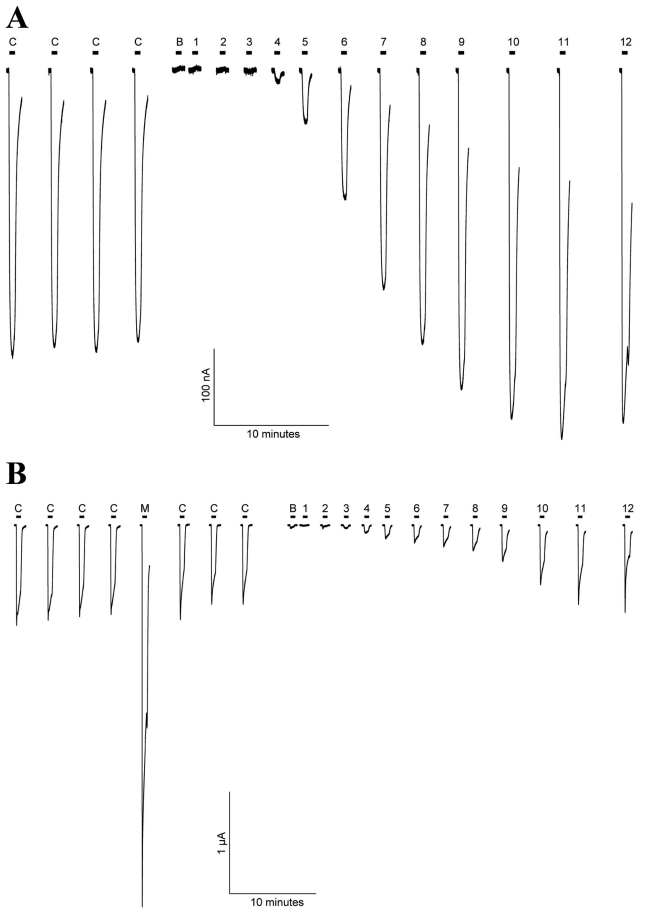

Figure 4. Representative current traces for ACh and NS3573 in two-electrode voltage-clamp electrophysiological experiments in *X. laevis* oocytes. ***A***, ACh concentration–response experiment in an oocyte injected with α4 and β2 nAChR subunits in a 1:4 ratio (representing a low-current amplitude experiments). ***B***, NS3573 concentration–response experiment in an oocyte injected with α4 and β2 nAChR subunits in a 4:1 ratio (representing a high-current amplitude experiments). Application of compound is indicated by a bar above each trace, and "C" denotes an ACh control concentration of 1 μM (1:4 ratio) or 10 μM (4:1 ratio), "M" denotes a 3 mM ACh_{max} concentration, "B" denotes a buffer application, and the numbers 1–12 denote increasing concentrations of ACh or NS3573 in half-log unit increments with minimal concentration of 316 pM in the first application and maximal concentration of 100 μM in the last application.

sensitivity components were not significantly altered for the two agonists as determined by one-way ANOVA (ACh: $p = 0.54$, $F = 0.62$; NS3573: $p = 0.48$, $F = 0.73$).

In an additional attempt to ensure a uniform $(\alpha4)_3(\beta2)_2$ receptor population, we used concatenated α4 and β2 subunits. In addition to the previously published dimeric β2-6-α4 construct (Zhou et al., 2003), we have prepared a tetrameric β2-6-α4-9-β2-6-α4 construct, in which the numbers between subunits indicate

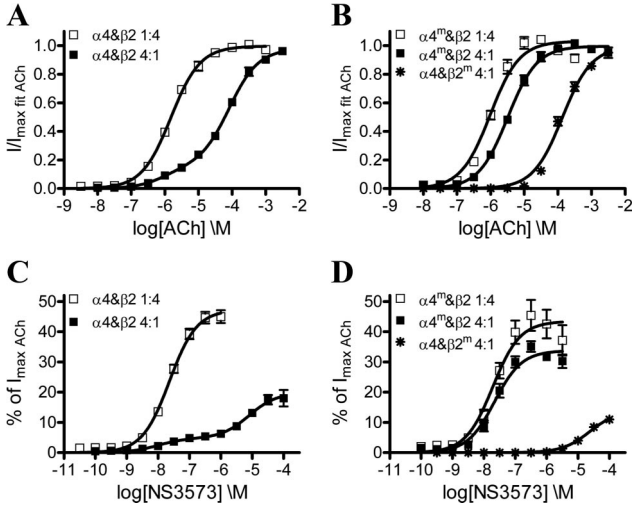

Figure 5. Functional concentration–response profiles of ACh and NS3573 on $\alpha4\beta2$ wild-type and mutant receptors. ***A***, ACh concentration–response curves from wild-type $\alpha4\beta2$ receptors expressed in 1:4 and 4:1 ratios. ***B***, ACh concentration–response curves on $\alpha4^{m}\beta2$ mutant receptors expressed in 1:4 and 4:1 ratios and $\alpha4\beta2^{m}$ mutant receptors expressed in a 4:1 ratio. ***C***, NS3573 concentration–response curves from wild-type $\alpha4\beta2$ receptors expressed in 1:4 and 4:1 ratios. ***D***, NS3573 concentration–response curves on $\alpha4^{m}\beta2$ mutant receptors expressed in 1:4 and 4:1 ratios and $\alpha4\beta2^{m}$ mutant receptors expressed in a 4:1 ratio. Data points are presented as mean ± SEM. Potencies, fractions of the high-sensitivity component on biphasic curves, number of experiments, and statistics are presented in Table 1.

the number of peptide linker AGS repeats. Both concatenated constructs were then expressed with $\alpha4$ subunits in a 1:1 weight ratio, and, given the absence of single $\beta2$ subunits, this should strongly favor assembly of receptors with the $(\alpha4)_3(\beta2)_2$ stoichiometry. Again, the data for both tested agonists are best fitted to a biphasic Hill equation (Fig. 6*C*,*D*,*G*,*H*; Table 1), and the fractions are not significantly different from those of the individual subunits expressed in a 4:1 ratio (ACh: $p = 0.16$ $F = 1.9$; NS3573: $p = 0.41$, $F = 0.90$). Control experiments with the tetrameric concatenated constructs and $\beta2$ subunit in a 1:1 ratio yield potencies for both agonists (Table 1) that are not significantly different from those obtained with the 1:4 ratio as determined by *t* test (ACh: $p = 0.15$, $t = 1.50$, df = 16; NS3573: $p = 0.30$, $t = 1.05$, df = 28). Comparing fractions from all datasets, in the attempts to obtain uniform $(\alpha4)_3(\beta2)_2$ receptor populations, by one-way ANOVA show that no single dataset has a fraction that is significantly different from the others (ACh: $p = 0.51$, $F = 0.83$; NS3573: $p = 0.56$, $F = 0.75$).

Converting the low-sensitivity $\alpha4\alpha4$ site into a high-sensitivity $\alpha4\beta2$-like site

If the low-sensitivity component of the biphasic responses obtained from $(\alpha4)_3(\beta2)_2$ receptors originates from agonist binding in the $\alpha4\alpha4$ site, it should in theory be possible to alter this component by mutating the $\alpha4\alpha4$ site to resemble an $\alpha4\beta2$ site. Thus, we expressed the above described $\alpha4^{m}$ triple mutant in 4:1 and 100:1 ratios with wild-type $\beta2$ to promote and ensure assembly of $(\alpha4^{m})_3(\beta2)_2$ receptors. Concentration–response datasets collected on the resulting receptor populations were best fitted to monophasic Hill equations, and the potencies obtained using the 4:1 ratio were 3.2 μM and 22 nM for ACh and NS3573, respectively, whereas the 100:1 ratio resulted in 3.8 μM and 27 nM (Fig. 5*B*,*D*; Table 1). This ACh potency was significantly different from that of $(\alpha4)_2(\beta2)_3$ receptors expressed in the 1:4 ratio ($p = 0.001$, $t = 4.27$, df = 12), albeit the actual difference is of low magnitude (1.6 μM vs 3.2 μM), whereas the potencies for NS3573 were not significantly different ($p = 0.85$, $t = 0.19$, df = 23). The (−)-side mutations of $\alpha4^{m}$ are also present in the two nonbinding $\beta2\alpha4$ interfaces (Fig. 1*A*), and, to investigate whether this affects receptor activation, we expressed $\alpha4^{m}$ and $\beta2$ in a 1:4 ratio. The resulting receptor population displayed monophasic responses to ACh and NS3573, which were virtually identical to those of wild-type $(\alpha4)_2(\beta2)_3$ receptors with potencies of 0.97 μM and 20 nM, respectively (Table 1).

Converting the high-sensitivity $\alpha4\beta2$ sites into low-sensitivity $\alpha4\alpha4$-like sites

The other way around, if the high-sensitivity component of the biphasic responses obtained from $(\alpha4)_3(\beta2)_2$ receptors originates from agonist binding in the $\alpha4\beta2$ sites, it should in theory be possible to alter this component by mutating the $\alpha4\beta2$ sites to resemble the $\alpha4\alpha4$ site. Thus, we expressed $\alpha4$ with the $\beta2^{m}$ triple mutant in a 4:1 ratio to promote assembly of $(\alpha4)_3(\beta2^{m})_2$ receptors. Again, the receptors displayed monophasic concentration–response curves for ACh and NS3573, but this time with potencies of 140 and 23 μM, respectively, resembling the low-sensitivity potency component of wild-type $(\alpha4)_3(\beta2)_2$ receptors (Fig. 5*B*,*D*; Table 1).

Discussion

Our results provide a novel explanation for the observation of two agonist sensitivities on $\alpha4\beta2$ nAChRs and on how they are related to different subunit stoichiometries. The $(\alpha4)_2(\beta2)_3$ receptor contains only one type of agonist binding site in the $\alpha4\beta2$ interfaces, giving rise to a monophasic response with high agonist sensitivity. The $(\alpha4)_3(\beta2)_2$ receptor contains two distinct agonist binding sites, and, as an intrinsic functional property, it results in biphasic concentration–response curves with high- and low-sensitivity components corresponding to agonist binding in the $\alpha4\beta2$ and $\alpha4\alpha4$ sites, respectively.

Comparing the $\alpha4\beta2$ and $\alpha4\alpha4$ sites

Comparison of our homology models showed that only three residues differ between the two sites and signify a local change from hydrophilic in the $\alpha4\alpha4$ site to more hydrophobic in the $\alpha4\beta2$ site (Fig. 3). The two sites are adequately similar for agonists to bind to both, but the three differing residues are expected to cause ligand-dependent differences in binding affinity between these two sites. The $(\alpha4)_2(\beta2)_3$ receptor, which only contains $\alpha4\beta2$ sites, display high agonist sensitivity toward ACh and NS3573, whereas the $(\alpha4)_3(\beta2)_2$ receptor that contains the $\alpha4\alpha4$ site additionally display low agonist sensitivity (Table 1). Considering the potencies as a first approximation of the binding affinities in the activated receptor state predicts that ACh and NS3573 display higher affinity for the $\alpha4\beta2$ sites and lower affinity for the $\alpha4\alpha4$ site. Along the same line, previous binding studies on $\alpha4\beta2$ receptors expressed in oocytes have indicated both high and low affinity binding sites for [^{3}H]epibatidine, with the majority of the sites displaying high affinity (Shafaee et al., 1999).

Biphasic $(\alpha4)_3(\beta2)_2$ concentration–response curves

In our initial experiments, we used 1:4 and 4:1 ratios between $\alpha4$ and $\beta2$ cRNA to obtain expression of $(\alpha4)_2(\beta2)_3$ and $(\alpha4)_3(\beta2)_2$ receptors, respectively. The receptors resulting from excess $\beta2$ display ACh and NS3573 concentration–response data that fit well to a monophasic Hill equation (Fig. 5*A*,*C*). Combined with the fact that the ACh potency is similar to what have been reported by others for $(\alpha4)_2(\beta2)_3$ (Moroni et al., 2006; Zwart et al.,

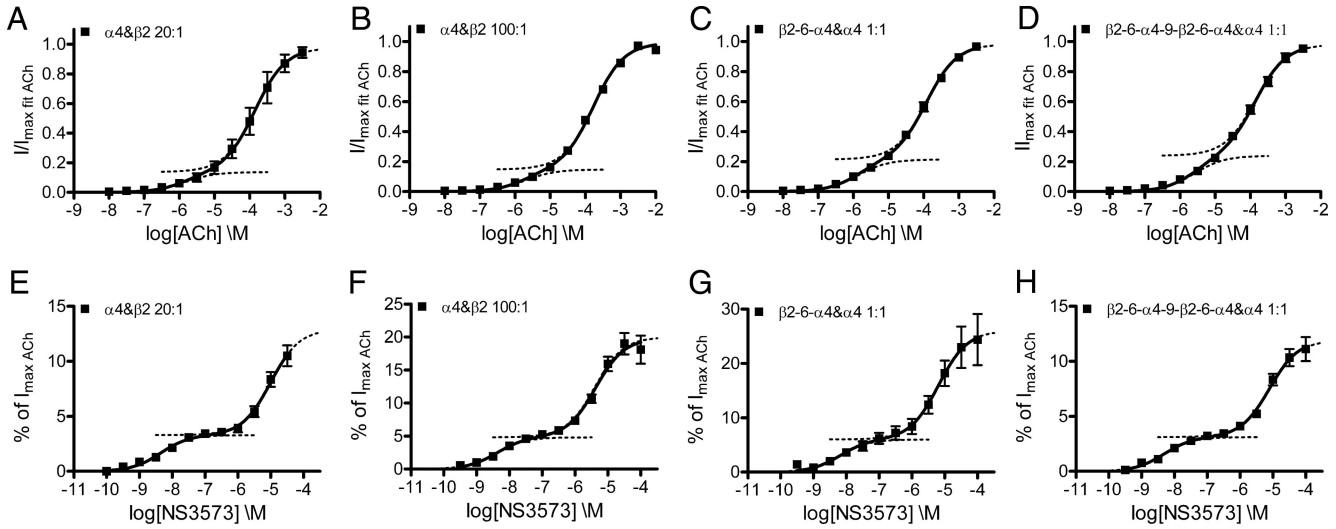

Figure 6. Functional concentration–response profiles for ACh and NS3573 on $\alpha4\beta2$ receptors with different subunit ratios or concatenated subunits. ***A***, ***B***, ACh concentration–response curves from $\alpha4\beta2$ receptors expressed in 20:1 and 100:1 ratios. ***C***, ACh concentration–response curve from $\alpha4\beta2$ receptors expressed from the dimeric concatenated $\beta2$-6-$\alpha4$ construct and $\alpha4$ in a 1:1 ratio. ***D***, ACh concentration–response curve from $\alpha4\beta2$ receptors expressed from the tetrameric concatenated $\beta2$-6-$\alpha4$-9-$\beta2$-6-$\alpha4$ construct and $\alpha4$ in a 1:1 ratio. ***E***, ***F***, NS3573 concentration–response curves from $\alpha4\beta2$ receptors expressed in 20:1 and 100:1 ratios. ***G***, NS3573 concentration–response curve from $\alpha4\beta2$ receptors expressed from the dimeric concatenated $\beta2$-6-$\alpha4$ construct and $\alpha4$ in a 1:1 ratio. ***H***, NS3573 concentration–response curve from $\alpha4\beta2$ receptors expressed from the tetrameric concatenated $\beta2$-6-$\alpha4$-9-$\beta2$-6-$\alpha4$ construct and $\alpha4$ in a 1:1 ratio. Theoretical sigmoidal curves using the obtained fitted values are plotted as dotted lines to visualize the two fractions. Data points are presented as mean ± SEM. Potencies, fractions of the high-sensitivity component, number of experiments, and statistics are presented in Table 1.

2006; Carbone et al., 2009), it shows that a 1:4 $\alpha4$:$\beta2$ ratio is sufficient to obtain a uniform $(\alpha4)_2(\beta2)_3$ receptor population. The case is less clear-cut for the receptors resulting from excess $\alpha4$ because the concentration–response data for ACh and in particular NS3573 is best fitted to a biphasic Hill equation. Others have reported similar biphasic concentration–response curves from $(\alpha4)_3(\beta2)_2$ receptors but, even with a 10:1 $\alpha4$:$\beta2$ expression ratio, they concluded that the high-sensitivity component is attributable to a $(\alpha4)_2(\beta2)_3$ receptor contamination (Carbone et al., 2009).

If the biphasic concentration–response curves is attributable to coexistence of $(\alpha4)_3(\beta2)_2$ and $(\alpha4)_2(\beta2)_3$ receptors, one would expect the fraction of the high-potency component to diminish with increasing $\alpha4$:$\beta2$ expression ratios. However, as depicted in Figures 5*A* and 6, *A* and *B*, the ACh concentration–response curves obtained on receptors resulting from 4:1, 20:1, and 100:1 $\alpha4$:$\beta2$ expression ratios are very similar. The fraction of the high-sensitivity component does not decrease as we go to higher excess of $\alpha4$ but remains ~15% (Table 1), and there is no significant difference between the ACh datasets collected on receptors from 4:1 and higher $\alpha4$:$\beta2$ ratios. The same was confirmed with the much more biphasic concentration–response curves of NS3573 (Figs. 5*C*, 6*E*,*F*); the fraction of the high-sensitivity component is independent of the expression ratio and remains ~25% (Table 1).

Expression of concatenated $\alpha4\beta2$ dimers and tetramers in the presence of single $\alpha4$ subunits should exclusively favor assembly of functional $(\alpha4)_3(\beta2)_2$ monopentameric receptors as shown previously for the dimeric construct (Zhou et al., 2003). The resulting ACh and NS3573 concentration–response curves for concatenated constructs expressed with large molar excess of single $\alpha4$ subunits were not significantly different from each other or from the curves obtained with high $\alpha4$:$\beta2$ ratios (Fig. 6), and the fractions remained the same (Table 1).

These results show that our $(\alpha4)_3(\beta2)_2$ receptor populations are indeed uniform and that the biphasic response is an intrinsic functional property with partial activation at low agonist concentration and additional activation at high agonist concentration.

High- and low-sensitivity agonist sites

With respect to current levels in the oocyte experiments, the general picture is one of lower current levels in receptors that are of $(\alpha4)_2(\beta2)_3$ stoichiometry compared with receptors of $(\alpha4)_3(\beta2)_2$ stoichiometry regardless of whether wild-type or mutant subunits were used (Table 1). This clearly indicates that the mutant subunits do not dramatically affect expression compared to wild-type subunits. Furthermore, because $(\alpha4)_3(\beta2)_2$ receptors seem to display larger conductance than $(\alpha4)_2(\beta2)_3$ receptors (Nelson et al., 2003), the current levels likely reflects receptor stoichiometry, i.e., number of $\alpha4$ subunits, rather than different expression levels.

Interestingly, it turns out that the three residues that differ between the $\alpha4\beta2$ and $\alpha4\alpha4$ sites completely control the difference in agonist sensitivity between the two sites. By mutating three residues on the (−)-side of the $\alpha4$ subunit, we altered a low-sensitivity $\alpha4\alpha4$ agonist binding site to closely resemble a high-sensitivity $\alpha4\beta2$ site. Data from experiments with the mutant $(\alpha4^m)_3(\beta2)_2$ receptors using 4:1 and 100:1 expression ratios unequivocally showed an abolishment of any low-sensitivity component in the concentration–response curves, and the receptors displayed only high agonist sensitivity to both agonists tested (Fig. 5*B*,*D*; Table 1). The large mutant $\alpha4^m$ subunit surplus as well as general current levels indicate uniform $(\alpha4^m)_3(\beta2)_2$ receptor stoichiometry in these experiments. The monophasic high-sensitivity concentration–response curves could be explained by the lack of agonist binding in the mutated $\alpha4\alpha4$ interface and activation only through agonist binding to the two $\alpha4\beta2$ sites. However, because the three mutations were introduced to alter the low-sensitivity $\alpha4\alpha4$ site to closely resemble a high-sensitivity $\alpha4\beta2$ site, the most likely explanation is that the mutant $(\alpha4^m)_3(\beta2)_2$ receptor contains three activation sites with similar high agonist sensitivity. This is further supported by the

fact that receptors assembled from either wild-type or mutant $\alpha4$ subunits and $\beta2$ in a 4:1 ratio result in total average currents higher than that obtained with the opposite ratio (Table 1), indicating sufficient expression levels and activation via three agonist sites. In the reverse experiment, we mutated the corresponding three residues on the (−)-side of the $\beta2$ subunit to alter the high-sensitivity $\alpha4\beta2$ agonist binding sites to resemble a low-sensitivity $\alpha4\alpha4$ site. Concentration–response data for the resulting mutant $(\alpha4)_3(\beta2^m)_2$ receptors only display low agonist sensitivity corresponding to a receptor population containing only low-sensitivity agonist sites (Fig. 5*B*,*D*; Table 1).

These results clearly show that the $\alpha4\alpha4$ interface contains a novel third agonist site, which display low agonist sensitivity to ACh and NS3573, whereas the $\alpha4\beta2$ sites exhibit high agonist sensitivity. A physiological implication of the two distinct ACh binding sites in the $(\alpha4)_3(\beta2)_2$ receptor is a significantly broadened dynamic response range to the endogenous neurotransmitter ACh. As a consequence, the $(\alpha4)_3(\beta2)_2$ receptor has the built-in opportunity to respond at two different current levels depending on the ACh concentration in the synapse. Furthermore, the presence of a low-sensitivity agonist site in the $\alpha4\alpha4$ interface offers a possible explanation for the weak and infrequent ACh-induced responses observed from oocytes injected with only $\alpha4$ cDNA (Deneris et al., 1989).

Fitting the concentration–response data

A crucial part of the electrophysiological experiments is how the concentration-response data are fitted to monophasic or biphasic Hill equations and especially the use of fixed or variable parameters; the more variables allowed the more datasets fit "well" to monophasic Hill equations. Using variable parameters, which is a customary reported fitting routine, our ACh data from $(\alpha4)_3(\beta2)_2$ receptors can be fitted to monophasic Hill equations with low Hill slopes and bottom of curves different from zero. However, regardless of variable parameters, the best-model *F* test prefers biphasic fitting for the NS3573 data obtained on $(\alpha4)_3(\beta2)_2$ receptors at all the conditions we have tried. Assuming the same activation profile for ACh and NS3573, we decided to use a fitting procedure with fixed parameters (Hill slope = 1, bottom = 0) on a global scale, resulting in significantly better fits to biphasic Hill equations for ACh data obtained on $(\alpha4)_3(\beta2)_2$ receptors.

Based on our results, it is crucial to acknowledge that the $(\alpha4)_3(\beta2)_2$ receptors contains two different ligand binding sites, and we strongly argue for the importance of using fixed parameters in analyzing data from receptors of both stoichiometries.

Consequences of an additional agonist site in the $\alpha4\alpha4$ interface

For the first time, we present a detailed explanation for the observation of both high and low sensitivities for many agonists on the $\alpha4\beta2$ nAChRs, and the acknowledgment of a third agonist site in the $(\alpha4)_3(\beta2)_2$ receptor subtype provides new opportunities for drug discovery. Based on the comparison of our homology models, the structural differences between the $\alpha4\beta2$ and $\alpha4\alpha4$ sites appear to be sufficient for structure-based design of ligands selective for one site over the other. Ligands selective for the $\alpha4\alpha4$ site is of particular interest because they would specifically target the $(\alpha4)_3(\beta2)_2$ receptor subtype, which is the dominantly expressed subtype (~70–80%) in native rat brain (Shafaee et al., 1999) and thus may be the pharmacologically most relevant subtype. Furthermore, a compound that selectively binds to the $\alpha4\alpha4$ site should in theory function as an allosteric modulator with negligible efficacy on the $(\alpha4)_3(\beta2)_2$ receptor without an agonist present and with no effect on the $(\alpha4)_2(\beta2)_3$ receptor.

Single-channel measurements have implied that the $(\alpha4)_3(\beta2)_2$ receptor displays larger conductance than the $(\alpha4)_2(\beta2)_3$ receptor (Nelson et al., 2003), and the same has been reported for $(\alpha3)_3(\beta4)_2$ versus $(\alpha3)_2(\beta4)_3$ (Krashia et al., 2010). Combined with results obtained on homomeric receptors (Rayes et al., 2009), it seems to be a general mechanistic feature of the nAChRs that agonist binding to three sites results in maximal activation. This may also apply to other Cys-loop receptors, e.g., the $GABA_A$ receptors in which the accessory γ-subunit adds additional plasticity to the channel activation through the benzodiazepine binding site (Atack, 2005) and thus functions similarly to the third α subunit in the nAChRs.

As suggested above, affecting a specific receptor subpopulation by developing compounds that bind to a subunit interface, which is only present in the receptor subtype of interest, may be a meaningful drug discovery strategy for Cys-loop receptors in general. As illustrated by the number of drugs affecting the benzodiazepine binding site, this strategy has successfully been applied in development of modulators for the $GABA_A$ receptors.

References

Armougom F, Moretti S, Poirot O, Audic S, Dumas P, Schaeli B, Keduas V, Notredame C (2006) Expresso: automatic incorporation of structural information in multiple sequence alignments using 3D-Coffee. Nucleic Acids Res 34:W604–W608.

Atack JR (2005) The benzodiazepine binding site of $GABA_A$ receptors as a target for the development of novel anxiolytics. Expert Opin Investig Drugs 14:601–618.

Berman HM, Westbrook J, Feng Z, Gilliland G, Bhat TN, Weissig H, Shindyalov IN, Bourne PE (2000) The Protein Data Bank. Nucleic Acids Res 28:235–242.

Carbone AL, Moroni M, Groot-Kormelink PJ, Bermudez I (2009) Pentameric concatenated $(\alpha4)_2(\beta2)_3$ and $(\alpha4)_3(\beta2)_2$ nicotinic acetylcholine receptors: subunit arrangement determines functional expression. Br J Pharmacol 156:970–981.

Celie PH, van Rossum-Fikkert SE, van Dijk WJ, Brejc K, Smit AB, Sixma TK (2004) Nicotine and carbamylcholine binding to nicotinic acetylcholine receptors as studied in AChBP crystal structures. Neuron 41:907–914.

DeLano WL (2002) The PyMOL molecular graphics system, version 1.3. New York: Schrodinger.

Dellisanti CD, Yao Y, Stroud JC, Wang ZZ, Chen L (2007) Crystal structure of the extracellular domain of nAChR $\alpha1$ bound to α-bungarotoxin at 1.94 Å resolution. Nat Neurosci 10:953–962.

Deneris ES, Boulter J, Connolly J, Wada E, Wada K, Goldman D, Swanson LW, Patrick J, Heinemann S (1989) Genes encoding neuronal nicotinic acetylcholine receptors. Clin Chem 35:731–737.

Hansen SB, Sulzenbacher G, Huxford T, Marchot P, Taylor P, Bourne Y (2005) Structures of Aplysia AChBP complexes with nicotinic agonists and antagonists reveal distinctive binding interfaces and conformations. EMBO J 24:3635–3646.

Jensen AA, Frølund B, Liljefors T, Krogsgaard-Larsen P (2005) Neuronal nicotinic acetylcholine receptors: structural revelations, target identifications, and therapeutic inspirations. J Med Chem 48:4705–4745.

Jensen ML, Timmermann DB, Johansen TH, Schousboe A, Varming T, Ahring PK (2002) The β subunit determines the ion selectivity of the $GABA_A$ receptor. J Biol Chem 277:41438–41447.

Krashia P, Moroni M, Broadbent S, Hofmann G, Kracun S, Beato M, Groot-Kormelink PJ, Sivilotti LG (2010) Human $\alpha3\beta4$ neuronal nicotinic receptors show different stoichiometry if they are expressed in *Xenopus* oocytes or mammalian HEK293 cells. PLoS One 5:e13611.

Kuryatov A, Luo J, Cooper J, Lindstrom J (2005) Nicotine acts as a pharmacological chaperone to up-regulate human $\alpha4\beta2$ acetylcholine receptors. Mol Pharmacol 68:1839–1851.

Marks MJ, Meinerz NM, Drago J, Collins AC (2007) Gene targeting demonstrates that $\alpha4$ nicotinic acetylcholine receptor subunits contribute to expression of diverse [^{3}H]epibatidine binding sites and components of

biphasic $^{86}Rb^+$ efflux with high and low sensitivity to stimulation by acetylcholine. Neuropharmacology 53:390–405.

Mirza NR, Larsen JS, Mathiasen C, Jacobsen TA, Munro G, Erichsen HK, Nielsen AN, Troelsen KB, Nielsen EØ, Ahring PK (2008) NS11394 [3′-[5-(1-hydroxy-1-methyl-ethyl)-benzoimidazol-1-yl]-biphenyl-2-carbonitrile], a unique subtype-selective $GABA_A$ receptor positive allosteric modulator: in vitro actions, pharmacokinetic properties and in vivo anxiolytic efficacy. J Pharmacol Exp Ther 327:954–968.

Moroni M, Zwart R, Sher E, Cassels BK, Bermudez I (2006) $\alpha4\beta2$ nicotinic receptors with high and low acetylcholine sensitivity: pharmacology, stoichiometry, and sensitivity to long-term exposure to nicotine. Mol Pharmacol 70:755–768.

Moroni M, Vijayan R, Carbone A, Zwart R, Biggin PC, Bermudez I (2008) Non-agonist-binding subunit interfaces confer distinct functional signatures to the alternate stoichiometries of the $\alpha4\beta2$ nicotinic receptor: an $\alpha4$-$\alpha4$ interface is required for Zn^{2+} potentiation. J Neurosci 28:6884–6894.

Nelson ME, Kuryatov A, Choi CH, Zhou Y, Lindstrom J (2003) Alternate stoichiometries of $\alpha4\beta2$ nicotinic acetylcholine receptors. Mol Pharmacol 63:332–341.

Peters D, Olsen GM, Nielsen SF, Østergaard E (1999) Heteroaryl diazacycloalkanes as cholinergic ligands at nicotinic acetylcholine receptors. PCT Patent WO 99/21834.

Rayes D, De Rosa MJ, Sine SM, Bouzat C (2009) Number and locations of agonist binding sites required to activate homomeric Cys-loop receptors. J Neurosci 29:6022–6032.

Sali A, Blundell TL (1993) Comparative protein modelling by satisfaction of spatial restraints. J Mol Biol 234:779–815.

Shafaee N, Houng M, Truong A, Viseshakul N, Figl A, Sandhu S, Forsayeth JR, Dwoskin LP, Crooks PA, Cohen BN (1999) Pharmacological similarities between native brain and heterologously expressed $\alpha4\beta2$ nicotinic receptors. Br J Pharmacol 128:1291–1299.

Shen MY, Sali A (2006) Statistical potential for assessment and prediction of protein structures. Protein Sci 15:2507–2524.

Tapia L, Kuryatov A, Lindstrom J (2007) Ca^{2+} permeability of the $(\alpha4)_3(\beta2)_2$ stoichiometry greatly exceeds that of $(\alpha4)_2(\beta2)_3$ human acetylcholine receptors. Mol Pharmacol 71:769–776.

The UniProt Consortium (2011) Ongoing and future developments at the Universal Protein Resource. Nucleic Acids Res 39:D214–D219.

Timmermann DB, Grønlien JH, Kohlhaas KL, Nielsen EØ, Dam E, Jørgensen TD, Ahring PK, Peters D, Holst D, Chrsitensen JK, Malysz J, Briggs CA, Gopalakrishnan M, Olsen GM (2007) An allosteric modulator of the $\alpha7$ nicotinic acetylcholine receptor possessing cognition-enhancing properties in vivo. J Pharmacol Exp Ther 323:294–307.

Zhou Y, Nelson ME, Kuryatov A, Choi C, Cooper J, Lindstrom J (2003) Human $\alpha4\beta2$ acetylcholine receptors formed from linked subunits. J Neurosci 23:9004–9015.

Zwart R, Broad LM, Xi Q, Lee M, Moroni M, Bermudez I, Sher E (2006) 5-I A-85380 and TC-2559 differentially activate heterologously expressed $\alpha4\beta2$ nicotinic receptors. Eur J Pharmacol 539:10–17.